Paleoseismology and Global Positioning System: Earthquake-cycle effects and geodetic versus geologic fault slip rates in the Eastern California shear zone

Timothy H. Dixon, E. Norabuena — Rosenstiel School of Marine and Atmospheric Sciences, University of Miami, 4600 Rickenbacker Causeway, Miami, Florida 33149, USA
L. Hotaling — Department of Geological Sciences, University of Miami, Miami, Florida 33124, USA

ABSTRACT

Published slip rates for the Owens Valley fault zone in eastern California based on geodetic data and elastic half-space models (5–7 mm/yr) are faster than longer term geologic rates (2–3 mm/yr). We use Global Positioning System data spanning the central Owens Valley, a more realistic rheological model with an elastic upper crust over a viscoelastic lower crust and upper mantle, and paleoseismic data from adjacent faults, to show that this difference could reflect earthquake-cycle effects. We estimate a long-term rate (2.1 ± 0.7 mm/yr) and earthquake recurrence interval (2750 +350/−1000 yr) from the geodetic data, both in agreement with independent geologic estimates.

Keywords: GPS, earthquake cycle, paleoseismology, fault slip rates.

INTRODUCTION

Crustal deformation near active faults reflects both long-term fault slip rate and short-term interseismic strain accumulation and postseismic effects. Rheological models quantitatively relate geodetically measured short-term deformation to a fault's long-term slip rate. The simplest model assumes that Earth is a perfectly elastic half-space. Although fitting a variety of geodetic data, this model ignores the rheology of rocks hotter than the brittle-ductile transition temperature, typically reached below ~10–20 km depth. This material is better represented by viscoelastic rheology, and may exhibit time-dependent (e.g., earthquake cycle) effects.

The Owens Valley fault zone is the westernmost of three active fault zones comprising the Eastern California shear zone north of the Garlock fault (Fig. 1). The shear zone accommodates ~25% of total Pacific–North America motion (Dokka and Travis, 1990; Savage et al., 1990; Sauber et al., 1994). Published slip rates for the Owens Valley fault zone vary by a factor of three. Beanland and Clark (1994) inferred a Holocene slip rate of 2 ± 1 mm/yr (one standard error). By using data on offset stream channels, a recurrence-interval estimate from dated trench sections, and assuming periodic earthquakes, Lee et al. (2001) determined a Holocene rate of 1.8 ± 0.3 mm/yr. They also noted that slip on the nearby Lone Pine fault (0.8 ± 0.4 mm/yr) should be included in estimates of total slip across the valley, giving 2.6 ± 0.5 mm/yr. In contrast, geodetic data fit to elastic half-space models predict rates of 5–7 mm/yr (e.g., Gan et al., 2000; Miller et al., 2001). McClusky et al. (2001) used all available Global Positioning System (GPS) data and a three-dimensional half-space model; they obtained rates between 5.3 ± 0.7 and 4.6 ± 0.5 mm/yr for three segments of the Owens Valley–Airport Lake fault zones. Although most of these estimates overlap within 95% confidence limits (twice the uncertainty values just stated), there appears to be a systematic difference, geodetically estimated rates being faster than geologically estimated rates.

There are three possible explanations for this discrepancy. (1) Both approaches are correct, and the slip rate is changing rapidly with time. (2) There are systematic errors in the geologic and/or geodetic data. (3) The data are correct, but underlying assumptions for the geologic and/or geodetic approaches are in error, causing the data to be misinterpreted. (3a) For example, geologically estimated rates could be too slow if additional nearby active fault segments were missed, or surface offsets in alluvial valleys like Owens Valley tend to lag total offset at depth. (3b) Alternately, or in addition, geodetic rates could be incorrect if the rheological model (elastic half-space) is inappropriate.

We think that explanation 1 is unlikely given the relatively small difference in time scales for the geologic (Holocene) and geodetic (decadal) studies. For comparison, the kinematic boundary condition, Pacific–North American plate motion, has been steady for the past 3 m.y. to within ~1 mm/yr (DeMets and Dixon, 1999). The previously cited independent geologic and geodetic studies give internally consistent results, suggesting that explanation 2 is also unlikely. Explanation 3a is possible, but difficult to evaluate with currently available data. Dixon et al. (2000) suggested that the discrepancy between geodetic and geologic rates here might reflect, at least in part, the influence of a viscoelastic lower crust and upper mantle, and corresponding earthquake-cycle effects not predicted by elastic half-space models. Dixon et al. (2000) also used a rheological model incorporating viscoelasticity to test direct estimation of paleoseismic parameters from geodetic data, based on limited GPS data in northern Owens Valley. A comprehensive GPS data set spanning central Owens Valley is now available, enabling more rigorous tests of explanation 3b and its corollary, paleoseismic parameter estimation with geodesy.

VISCOELASTIC COUPLING MODEL

Viscoelastic coupling models, with an elastic layer overlying one or more viscoelastic layers, can explain transient crustal deformation after an earthquake (e.g., Thatcher, 1983; Li and Rice, 1987; Pollitz and Sacks, 1992). Savage and Lisowski (1998) presented a model for a single vertical strike-slip fault in an elastic layer (brittle upper crust) of thickness h over a viscoelastic half space (ductile lower crust and upper mantle) (Fig. 2). We use this model to approximate the rheology of our study area. The half space is a Maxwell viscoelastic solid, the mechanical analogue of which is a spring and dashpot in series. Its physical properties are specified by the rigidity, μ (the spring), and

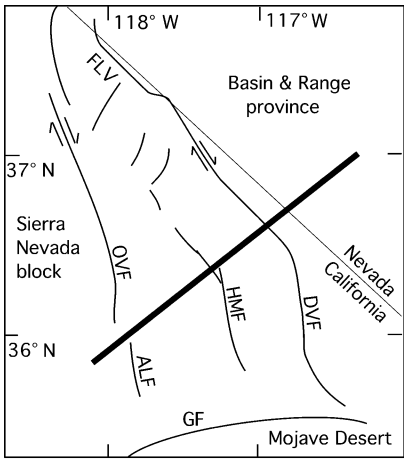

Figure 1. Sketch map of study area, modified from Dixon et al. (1995). Bar marks approximate location of Global Positioning System transect (Gan et al., 2000). GF—Garlock fault. Labeled faults of Eastern California shear zone: ALF—Airport Lake fault zone; OVF—Owens Valley fault zone; HMF—Hunter Mountain–Panamint Valley fault zone; DVF—Death Valley–Furnace Creek fault zone; FLV—Fish Lake Valley fault zone.

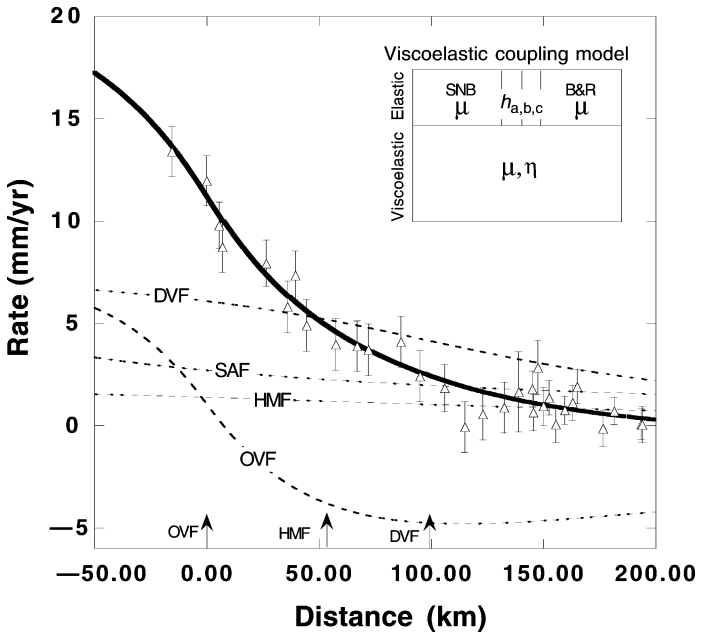

Figure 2. Global Positioning System velocity (triangles) and one standard error (bars) from Gan et al. (2000) compared to prediction of viscoelastic coupling model (heavy solid line), representing summed velocity contributions from four parallel faults (light dashed lines). SAF—San Andreas fault; DVF—Death Valley–Furnace Creek fault zone; HMF—Hunter Mountain–Panamint Valley fault zone; OVF—Owens Valley fault zone. Inset shows model rheology for Eastern California shear zone. SNB—Sierra Nevada block; B&R—Basin and Range Province; *h* is fault depth (depth of elastic layer) for three faults (a, b, or c), μ is rigidity, η is viscosity. Arrows mark location of major shear-zone faults.

viscosity, η (the dashpot). The Maxwell time τ is η/μ (or 2η/μ to account for the half-space). When this system is stressed, the elastic behavior of the spring dominates on time scales shorter than τ, but the viscous behavior of the dashpot takes over on time scales longer than τ. Typical Maxwell times for Earth materials range from years to hundreds of years. For simplicity, the elastic and viscoelastic materials are assumed to have the same rigidity.

The main transient stresses in this model come from earthquakes, when the upper elastic layer slips by large amounts. The adjacent ductile region, stimulated by upper layer motion, flows in the direction of coseismic slip during the postseismic phase, which may last many Maxwell times. The flowing ductile material in turn imparts a traction on the base of the upper layer in the direction of fault motion, resulting in a high surface velocity gradient near the fault early in the earthquake cycle and a narrow zone of strain accumulation. With time, the high-velocity, high-stress zone near the fault diffuses outward, broadening the zone of strain accumulation and lowering near-fault velocity gradients (Fig. 2).

APPLICATION TO THE EASTERN CALIFORNIA SHEAR ZONE

GPS data from Gan et al. (2000) define a velocity transect perpendicular to plate motion spanning the Eastern California shear zone near central Owens Valley, California (Fig. 2). We used all available data from sites within 20 km of the transect, except site G005, an outlier probably reflecting local deformation at the Coso geothermal field, giving 31 rate estimates. Following Gan et al. (2000), we calculated the rate component parallel to N36°W—the local plate-motion direction and approximately parallel to the average strike of major strike-slip faults in the area—and corresponding uncertainties.

From west to east the active faults here are the Owens Valley, the Hunter Mountain–Panamint Valley, and the Death Valley–Furnace Creek fault zones. Strain from the San Andreas fault to the west, the main plate boundary, must also be considered. Ideally we would use a three-dimensional model with laterally varying rheology and multiple fault segments to address this problem. Unfortunately, such models are not yet available. We assume instead that the velocity contributions of the individual faults can be calculated separately in the coupling model and summed, ignoring fault interactions and laterally varying rheology. This ''principle of linear superposition,'' appropriate for elastic rheology, is an oversimplification for the coupling model. In addition, the coupling model only accounts for the strike-slip component of motion, although all three shear-zone fault zones have both strike-slip and dip-slip motion. However, the dip-slip component is relatively small compared to the strike-slip component (Dixon et al., 2000).

We compare the GPS velocity data to the velocity predicted by the coupling model for four parallel faults. We fixed most of the parameters on the basis of additional information (Table 1) and adjusted four parameters in a forward-modeling (grid search) approach, minimizing misfit between data and model (see Dixon et al. [2000] for details). We adjusted slip rate and earthquake recurrence interval for the Owens Valley fault zone (the last earthquake was in A.D. 1872) and slip rate and time of last earthquake for the Death Valley–Furnace Creek fault zone. The model is not sensitive to the recurrence interval for this fault, and we arbitrarily set it to 500 yr. For the Hunter Mountain–Panamint Valley fault zone, we fixed the slip rate and earthquake recurrence interval (Zhang et al., 1990) (Table 1) and arbitrarily set the time of the last earthquake such that the fault is in the middle of its earthquake cycle, essentially equivalent to the elastic half-space approximation. The model is not very sensitive to this parameter. To partially account for the known rheological asymmetry in the region (Malservisi et al., 2001), we set the depth of the elastic layer to 12 km for the San Andreas fault (Savage and Lisowski, 1998) and 10 km beneath the three eastern faults. We determined half-space viscosity as

TABLE 1. FIXED AND ADJUSTED PARAMETERS, VISCOELASTIC COUPLING MODEL

	San Andreas fault	Owens Valley fault zone	Hunter Mtn–Panamint Valley fault zone	Death Valley–Furnace Creek fault zone
Rate (mm/yr)	34*	**2.1 ± 0.3**	2.4†	**8.3 ± 1.2**
Elastic layer thickness (km)	12*	10	10	10
Recurrence interval (yr)	206*	**2750 ± 300**	1350†	500
Last earthquake (yr A.D.)	1857*	1872§	1325#	**1750** $^{+50}_{-150}$
Viscosity (Pa s)	3 x 10^{19}	1 x 10^{19}	1 x 10^{19}	1 x 10^{19}
Rigidity (Pa)	3 x 10^{10}	3 x 10^{10}	3 x 10^{10}	3 x 10^{10}

Note: Four adjusted parameters listed in **bold** type. Uncertainties assume $\chi^2_{95\%} = \chi^2_{best}\{1 + [\nu_1 \div (\nu_2 - \nu_1)]F\}$, where χ^2_{best} is the best-fit χ^2 (17.7), ν_1 is the number of adjusted parameters (4), ν_2 is the number of data (31), and F is the F ratio statistic at $F(.05)_{\nu1, \nu2}$. This estimate does not account for uncertainty in other parameters. To partly compensate we take the uncertainties listed above to represent one standard error.

* Working Group on California Earthquake Probabilities (1995).

† Holocene rate and recurrence interval from Zhang et al. (1990), assuming periodic earthquakes and most recent offset (3.2 m).

§ Beanland and Clark (1994).

#Assumes fault is in middle of earthquake cycle.

follows. For the San Andreas fault, we set the viscosity to 3×10^{19} Pa·s, from postseismic response to the 1906 San Francisco earthquake (Kenner and Segall, 2000). For the shear-zone region, 3×10^{19} Pa·s is an upper bound because heat flow is higher in the Basin and Range Province than in the San Andreas region of northern California. A lower bound can be estimated from studies of the Mojave Desert, a region with heat flow similar to that of our study area. Pollitz et al. (2000) estimated a viscosity of 8×10^{18} Pa·s for the upper mantle beneath the Mojave Desert, with lower-crustal viscosity a factor of two higher. Our model represents the lower crust and upper mantle as a single unit; hence our half-space viscosity reflects an average of lower crust and upper mantle values, and 8×10^{18} Pa·s is a lower bound. We fixed the viscosity of the half-space for the shear-zone faults to the intermediate value of 1×10^{19} Pa·s for most of the models, but also examined the effect of the upper and lower bounds.

Because the coupling model assumes laterally homogeneous rheology, our approach of summing velocity fields for several faults with different rheologies is not strictly valid. However, faults with different rheologies have velocity profiles that mainly differ in the near field (closer than ~100 km). The San Andreas fault is ~185 km away from the Owens Valley fault. The difference between the velocity due to the San Andreas fault calculated at Owens Valley with the already-stated assumptions and the velocity calculated with laterally uniform rheology (with the shear-zone values) is 0.9 mm/yr; the corresponding effect on the estimated Owens Valley slip rate is small. We also present models with laterally homogeneous rheology using the previously given extreme values, and incorporate the effect in our total uncertainty estimates.

We examined slip rates between 1 and 15 mm/yr and recurrence intervals between 200 and 4000 yr in 50 yr increments. We avoided unlikely parameter combinations, e.g., recurrence intervals shorter than time since the last earthquake, or slip-rate and recurrence-interval combinations that imply large (>15 m) coseismic offset in future earthquakes (the largest known surface offset, from the 1931 Fuyun earthquake in China, may be as high as 14.8 m; Lin and Lin, 1998). Thus, our model honors all available geologic data.

RESULTS AND DISCUSSION

Parameter estimates are listed in Table 1. The χ^2 per degree of freedom (31 rate data, four adjusted parameters) for the minimum misfit model is 0.65, better than the expected value of 1.0 for acceptable model fit and realistic data uncertainties. All data fit the model within 95% confidence (twice the standard error); all but three rate datums fit the model within one standard error (Fig. 2). The estimated slip rate of the Owens Valley fault zone is 2.1 ± 0.3 mm/yr, significantly slower than previous geodetic estimates employing elastic half-space models, but equivalent to published geologic estimates (Fig. 3A). The difference may reflect the fact that the Owens Valley fault is in the early stages of its earthquake cycle, when near-fault velocity gradients are higher than predicted by elastic half-space models. For most of the earthquake cycle, viscoelastic coupling models and elastic half-space models should yield similar slip-rate estimates.

Our slip-rate estimate for the Owens Valley fault zone depends on the assumed viscosity, and this dependence is not reflected in the uncertainty previously discussed. However, for the tested range of viscosities, all the slip-rate estimates are slower than published geodetic estimates with elastic half-space rheology. For example, assuming laterally homogeneous rheology, we obtain 2.6 mm/yr for a viscosity of 8×10^{18} Pa·s and locking depth of 10 km, and 1.8 mm/yr for a viscosity of 3×10^{19} Pa·s and locking depth of 12 km. Incorporating the rheologic uncertainty increases the total slip-rate uncertainty to ~0.7 mm/yr, but these rate estimates are nevertheless slower than geodetic elastic half-space estimates at 95% confidence. We conclude that earthquake cycle effects and viscoelastic rheology of the lower crust and upper mantle can affect fault slip rates estimated from geodetic data, providing a viable explanation for the discrepancy between geologic and previous geodetic estimates for the Owens Valley fault slip rate.

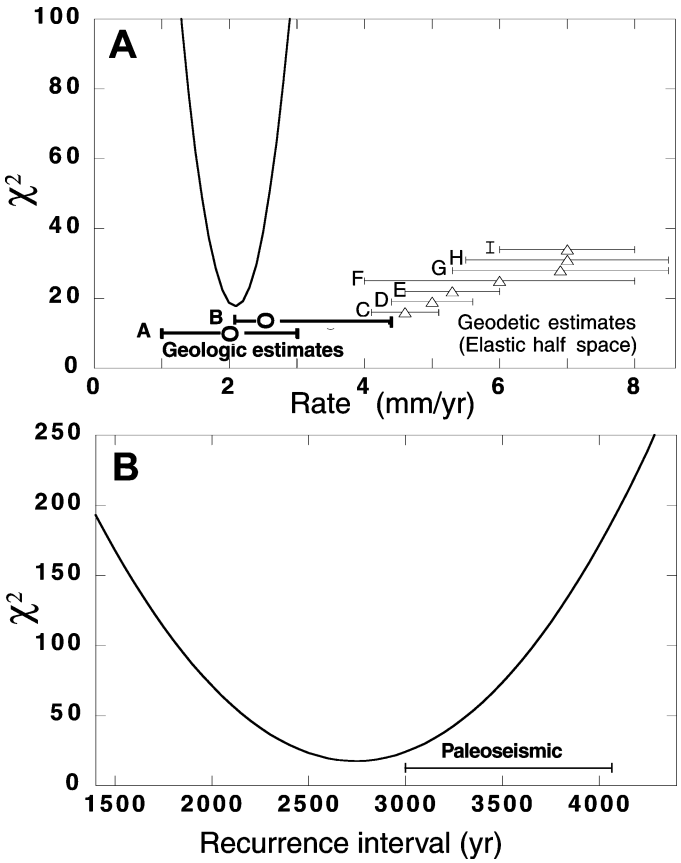

Figure 3. A: χ^2 misfit vs. slip rate for Owens Valley fault zone; other parameters are fixed to best-fitting values. Minimum misfit indicates best estimate (2.1 mm/yr). References for geologic (circles, heavy solid lines) and other geodetic estimates (triangles, thin lines, Global Positioning System data unless noted) and approximate one standard error, with arbitrary vertical location: A—Beanland and Clark (1994); B—Lee et al. (2001), 2.6 ± 0.5 mm/yr, including Lone Pine fault, and increased upper limit (4.4 mm/yr) to account for possible nonuniform recurrence; C–E—McClusky et al. (2001) for Owens Valley and Airport Lake faults; F—Dixon et al. (2000) for northern Owens Valley; G—Gan et al. (2000); H—Miller et al. (2001), uncertainty arbitrarily taken as 1.5 mm/yr; I—Savage and Lisowski (1995), electronic distance measurement. B: Similar to A, for recurrence interval. Horizontal bar represents range of paleoseismic data (Lee et al., 2001).

Our results imply relatively fast slip on the Death Valley–Furnace Creek fault zone, 8.3 ± 1.2 mm/yr (+1.2/−3.3 mm/yr, incorporating the rheologic uncertainty), presumably detectable with geologic studies. If we assign a higher rate to the Hunter Mountain–Panamint fault zone (e.g., Sternloff, 1988), the estimated rate on the Death Valley fault zone is reduced accordingly, because there is a trade-off between these two parameters (stated uncertainties do not reflect these trade-offs). Reheis and Sawyer (1997) reported an average rate of 9.5 +2.2/−3.1 mm/yr for the past 620 k.y. for the Oasis segment of the Fish Lake Valley fault zone, the northwest continuation of the Death Valley–Furnace Creek fault zone, consistent with our result. However these authors also noted that the rate may be slowing with time. Another test involves comparing the summed slip rates for the three shear-zone faults on the transect (12.8 mm/yr), plus slip on the San Andreas fault (34 mm/yr), plus slip on faults west of the San Andreas (2.0 mm/yr; Sorlien et al., 1999), for a total rate of 48.8 mm/yr, to the total Pacific–North Amer-

ican plate rate predicted by an independent model. Because the faults strike approximately parallel to plate motion, the two rates should be the same, unless there are additional active structures missed in the transect. Using the geologic model of DeMets and Dixon (1999), independent of GPS data, we predict 49.2 mm/yr of total Pacific–North America motion, calculated at 35°N on the San Andreas fault. The two rates are equivalent within uncertainties.

Figure 3B shows data misfit as a function of earthquake recurrence interval for the Owens Valley fault zone. The data and model have some sensitivity to this parameter because the fault is early in its earthquake cycle. Beanland and Clark (1994) noted that average slip in 1872 was 6 ± 2 m and maximum slip was 10 m. If earthquakes are periodic, the range of possible recurrence intervals, using published slip rates for this fault and their uncertainties at one standard error, is 500 yr (4 m at 8 mm/yr) to 10 k.y. (10 m at 1 mm/yr). The trenching data of Lee et al. (2001) indicate a recurrence interval between 3000 and 4100 yr, equivalent within uncertainties to our geodetic prediction, 2750 ± 300 yr (+350/−1000 yr, including the rheologic uncertainty). It is also possible to estimate other parameters with the model, rather than fixing them to known or assumed values. For example, we can estimate the date of the last earthquake for the Owens Valley fault (in 25 yr increments) rather than fixing it to the known value (1872) and adjusting the other four parameters as before. We obtain A.D. 1875 ± 50 for all tested rheologies. Thus, in cases where historical data are unavailable, it may be possible to determine the date of the last earthquake from geodetic data.

There are limitations to our model. Misfit is higher near the faults than elsewhere (Fig. 2), suggesting unmodeled near-fault processes. We do not represent segmentation and three-dimensional geometry of faults, or their interactions, and assume strictly periodic earthquakes. Lithospheric rheology is more complex than our two-layer, laterally homogeneous model, in both a vertical (Pollitz et al., 2000) and horizontal (Malservisi et al., 2001) sense. Despite these limitations, the simple coupling model is a more realistic representation of rheology than the elastic half-space model, predicts a velocity profile across the Eastern California shear zone that agrees with GPS data, and predicts a slip rate and earthquake recurrence interval for the Owens Valley fault zone that agrees with independent geologic data. Perhaps the most important result of our study is to highlight the importance of rheology and seismic cycle effects when interpreting geodetic data near active faults. A broader understanding of fault processes will require joint consideration of geodetic and paleoseismic data, realistic rheology, and seismic, heat flow, laboratory, and other data.

ACKNOWLEDGMENTS

We thank Fred Pollitz, Jim Savage, Wayne Thatcher, Marith Reheis, and Meghan Miller for discussions. Jeff Lee, Carol Prentice, Kevin Furlong, Wayne Thatcher, and Tom Gardner provided thoughtful reviews that greatly improved the manuscript. This work was supported by National Science Foundation grant EAR-0003740, the National Aeronautical and Space Administration, and the Office of Naval Research.

REFERENCES CITED

Beanland, S., and Clark, M.M., 1994, The Owens Valley fault zone, eastern California, and surface faulting associated with the 1872 earthquake: U.S. Geological Survey Bulletin, v. 1982, 29 p.

DeMets, C., and Dixon, T.H., 1999, New kinematic models for Pacific North America motion from 3 Ma to present: Evidence for steady motion and biases in the NUVEL-1A model: Geophysical Research Letters, v. 26, p. 1921–1924.

Dixon, T.H., Robaudo, S., Lee, J., and Reheis, M.C., 1995, Constraints on present-day Basin and Range deformation from space geodesy: Tectonics, v. 14, p. 755–772.

Dixon, T.H., Miller, M., Farina, F., Wang, H., and Johnson, D., 2000, Present-day motion of the Sierra Nevada block and some tectonic implications for the Basin and Range province, North American Cordillera: Tectonics, v. 19, p. 1–24.

Dokka, R.K., and Travis, C.J., 1990, Role of the Eastern California shear zone in accommodating Pacific–North American plate motion: Geophysical Research Letters, v. 17, p. 1323–1326.

Gan, W., Svarc, J.L., Savage, J.C., and Prescott, W.H., 2000, Strain accumulation across the eastern California shear zone at 36°30′N: Journal of Geophysical Research, v. 105, p. 16,229–16,236.

Kenner, S.J., and Segall, P., 2000, Post-seismic deformation following the 1906 San Francisco earthquake: Journal of Geophysical Research, v. 105, p. 13,195–13,209.

Lee, J., Spencer, J., and Owen, L., 2001, Holocene slip rates along the Owens Valley fault, California: Implications for the recent evolution of the eastern California shear zone: Geology, v. 29, p. 819–822.

Li, V.C., and Rice, J.R., 1987, Crustal deformation in great California earthquakes: Journal of Geophysical Research, v. 92, p. 11,533–11,551.

Lin, A., and Lin, S., 1998, Tree damage and surface displacement: The 1931 M 8.0 Fuyun earthquake: Journal of Geology, v. 106, p. 751–757.

Malservisi, R., Furlong, K.P., and Dixon, T.H., 2001, Influence of the earthquake cycle and lithospheric rheology on the dynamics of the eastern California shear zone: Geophysical Research Letters, v. 28, p. 2731–2734.

McClusky, S., Bjornstad, S.C., Hager, B.H., King, R.W., Meade, B.J., Miller, M.M., Monastero, F.C., and Souter, B.J., 2001, Present-day kinematics of the eastern California shear zone from a geodetically constrained block model: Geophysical Research Letters, v. 28, p. 3369–3372.

Miller, M.M., Johnson, D., Dixon, T.H., and Dokka, R.K., 2001, Refined kinematics of the eastern California shear zone from GPS: Journal of Geophysical Research, v. 106, p. 2245–2263.

Pollitz, F.F., and Sacks, I.S., 1992, Modeling of postseismic relaxation following the great 1857 earthquake, southern California: Seismological Society of America Bulletin, v. 82, p. 454–480.

Pollitz, F.F., Peltzer, G., and Bürgmann, R., 2000, Mobility of continental mantle: Evidence from post-seismic geodetic observation following the 1992 Landers earthquake: Journal of Geophysical Research, v. 105, p. 8035–8054.

Reheis, M.C., and Sawyer, T.L., 1997, Late Cenozoic history and slip rates of the Fish Lake Valley, Emigrant Peak and Deep Springs fault zones, Nevada and California: Geological Society of America Bulletin, v. 109, p. 280–299.

Sauber, J., Thatcher, W., Solomon, S., and Lisowski, M., 1994, Geodetic slip rate for the eastern California shear zone and the recurrence time of Mojave Desert earthquakes: Nature, v. 367, p. 264–266.

Savage, J.C., and Lisowski, M., 1995, Strain accumulation in Owens Valley: Seismological Society of America Bulletin, v. 85, p. 151–158.

Savage, J.C., and Lisowski, M., 1998, Viscoelastic coupling model of the San Andreas fault along the big bend, southern California: Journal of Geophysical Research, v. 103, p. 7281–7292.

Savage, J.C., Lisowski, M., and Prescott, W.H., 1990, An apparent shear zone trending north-northwest across the Mojave Desert into Owens Valley: Geophysical Research Letters, v. 17, p. 2113–2116.

Sorlien, C.C., Kamerling, M., and Mayerson, D., 1999, Block rotation and termination of the Hosgri fault, California, from 3-D map restoration: Geology, v. 27, p. 1039–1042.

Sternloff, K.R., 1988, Structural style and kinematic history of the active Panamint-Saline extensional system, Inyo county, California [Ph.D. thesis]: Cambridge, Massachusetts Institute of Technology, 30 p.

Thatcher, W., 1983, Nonlinear strain buildup and the earthquake cycle on the San Andreas fault: Journal of Geophysical Research, v. 88, p. 5893–5902.

Working Group on California Earthquake Probabilities, 1995, Seismic hazards in southern California earthquakes, 1994–2024: Seismological Society of America Bulletin, v. 85, p. 379–439.

Zhang, P., Ellis, M., Slemmons, D., and Mao, F., 1990, Right lateral displacements and Holocene slip rate associated with prehistoric earthquakes along the southern Panamint Valley fault zone: Journal of Geophysical Research, v. 95, p. 4857–4872.

Manuscript received June 13, 2002
Revised manuscript received September 20, 2002
Manuscript accepted September 24, 2002

Printed in USA